CHAPTER TEN

Preparation of carotenoid cleavage dioxygenases for X-ray crystallography

Anahita Daruwalla[a,†], **Xuewu Sui**[b,c,†], **and Philip D. Kiser**[a,d,e,†,*]

[a]Department of Physiology & Biophysics, University of California, Irvine School of Medicine, Irvine, CA, United States
[b]Department of Molecular Metabolism, Harvard T.H. Chan School of Public Health, Boston, MA, United States
[c]Department of Cell Biology, Harvard Medical School, Boston, MA, United States
[d]Department of Ophthalmology, Center for Translational Vision Research, University of California, Irvine School of Medicine, Irvine, CA, United States
[e]Research Service, VA Long Beach Healthcare System, Long Beach, CA, United States
*Corresponding author: e-mail address: pkiser@uci.edu

Contents

† These authors contributed equally to this work.

Methods in Enzymology, Volume 671
ISSN 0076-6879
https://doi.org/10.1016/bs.mie.2021.10.020

Abstract

Carotenoid cleavage dioxygenases (CCDs) constitute a superfamily of enzymes that are found in all domains of life where they play key roles in the metabolism of carotenoids and apocarotenoids as well as certain phenylpropanoids such as resveratrol. Interest in these enzymes stems not only from their biological importance but also from their remarkable catalytic properties including their regioselectivity, their ability to accommodate diverse substrates, and the additional activities (e.g., isomerase) that some of these enzyme possess. X-ray crystallography is a key experimental approach that has allowed detailed investigation into the structural basis behind the interesting biochemical features of these enzymes. Here, we describe approaches used by our lab that have proven successful in generating single crystals of these enzymes in resting or ligand-bound states for high-resolution X-ray diffraction analysis.

1. Introduction

Proteins of the carotenoid cleavage dioxygenase (CCD) superfamily are the dominant enzymes in nature responsible for converting carotenoid and apocarotenoid substrates into smaller apocarotenoid products. Apart from this well-known function, certain CCD subfamilies display alternative substrate preferences, the best characterized of which is the stilbenoid-cleaving dioxygenase group, the members of which cleave phenylpropanoid compounds such as resveratrol and lignostilbene (Brefort et al., 2011; Kamoda & Saburi, 1993). Some CCDs also exhibit activities ancillary to the double bond cleavage including structural and geometric isomerizations of the carotenoid backbone (Bruno et al., 2017; Oberhauser, Voolstra, Bangert, von Lintig, & Vogt, 2008). Finally, the RPE65 subfamily of CCDs does not function physiologically to cleave double bonds, but instead catalyzes the formation of 11-*cis*-retinol from all-*trans*-retinyl

palmitate (Moiseyev et al., 2006; Redmond et al., 2005). CCDs are expressed in organisms from all domains of life and are widely found in nature (Kiser, 2019). Although CCDs exist in organisms that diverged from one another eons ago, these enzymes are united by a conserved iron binding motif consisting of an inner sphere of four His residues and an anionic outer sphere of three Glu (or Asp) residues that maintain the structure of the inner sphere His ligands (Kloer, Ruch, Al-Babili, Beyer, & Schulz, 2005). Spectroscopy studies show that CCDs typically have a five coordinated $Fe^{(II)}$ center in their resting states (Daruwalla et al., 2020; Sui et al., 2017) as opposed to the typical six-coordinated geometry seen in other mononuclear non-heme iron oxygenases (Neidig & Solomon, 2005).

Key features of CCDs are their characteristic stereo- and regioselectivities toward their substrates (Daruwalla & Kiser, 2020). Identification of a 9-*cis*-epoxycarotenoid dioxygenase, VP14 from the plant *Zea mays* (Schwartz, Tan, Gage, Zeevaart, & McCarty, 1997), paved the way for the molecular characterization and cloning of CCDs from fungi, metazoans, and bacteria (Prado-Cabrero, Scherzinger, Avalos, & Al-Babili, 2007; Ruch, Beyer, Ernst, & Al-Babili, 2005; von Lintig & Vogt, 2000; Wyss et al., 2000) as well as other plant CCDs (Auldridge et al., 2006). These CCDs cleave at specific sites along the polyene chain of their substrates resulting in the generation of apocarotenoid products with diverse physiological roles, ranging from the hormone action of abscisic acid in plants to the light-sensing function of retinal and its isomers in bacteria and animals.

The crystallographic structure of an apocarotenoid forming CCD from *Synechocystis* sp. PCC 6803 (*Syn*ACO), first revealed the basic CCD fold consisting of a 7-bladed beta propeller base capped by a mostly alpha-helical dome (Kloer et al., 2005). Other CCD structures studied since then, such as the plant CCD, VP14 (Messing et al., 2010), and stilbenoid-cleaving oxygenases (SCOs) like *Neurospora crassa* CAO1 (Sui et al., 2017) and *Novosphingobium aromaticivorans* NOV1 (McAndrew et al., 2016), the archaeal enzyme *Nitrosotalea devanaterra* CCD (*Nd*CCD) (Daruwalla et al., 2020), and RPE65 (Kiser, Golczak, Lodowski, Chance, & Palczewski, 2009) have shown that all members of the family exhibit a similar beta propeller fold but with significant variation in the structure of the helical dome which confers specific properties such as substrate specificity and membrane affinity (Fig. 1). The heterologous expression of carotenoid-cleaving CCDs in bacterial systems can be complicated by their intrinsic hydrophobicity that arises from solvent-exposed lipophilic patches. Additionally, CCDs are prone to misfolding during heterologous expression in *E. coli*

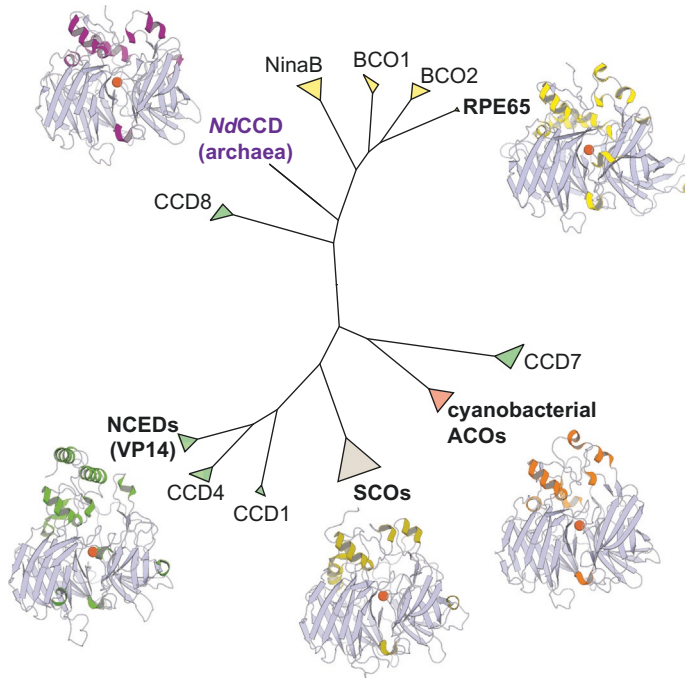

Fig. 1 A CCD phylogeny and representative crystal structures from the different subfamilies. The Bayesian phylogeny shows major groups of CCDs from plants (light green triangles), cyanobacteria (orange triangle), metazoans (yellow triangles), and the mixed bacterial/fungal SCO group (olive triangle). Also shown in purple text is an archaeal CCD from *Nitrosotalea devanaterra*, *Nd*CCD. Groups for which at least one crystal structure has been determined are shown in bold. The crystal structures shown are as follows with PDB accession codes given in parentheses: bovine RPE65 (4F2Z), *Syn*ACO (4OU9), *Neurospora crassa* CAO1 (5U8X), *Zea mays* VP14 (3NPE), and *Nd*CCD (6VCF).

(Kiser, Lodowski, & Palczewski, 2007; Kloer et al., 2005). Because SCOs lack exposed hydrophobic patches and cleave substrates with relatively greater water solubility than (apo)carotenoids, these enzymes are more amenable to detailed structural and spectroscopic analysis and thus serve as important model systems for studying CCD catalysis in general (Sui et al., 2017). Although the field has advanced substantially since the first 3D structure of a CCD was elucidated, there are several subfamilies of CCDs that remain to be structurally characterized to fully understand the enzymes' chemistry and biology (Fig. 1).

This chapter describes methods we have developed to express, purify, characterize and crystallize CCDs for analysis by X-ray crystallography. The methods we describe are also applicable to produce CCDs for other applications including various spectroscopic approaches.

2. Methods overview

The first successful structure determination of a CCD was reported in 2005 by the Schulz laboratory (Kloer et al., 2005). This group studied the apocarotenoid-cleaving enzyme *Syn*ACO, also known as Diox1 (NCBI accession code BAA18428) (Ruch et al., 2005). In this study, *Syn*ACO was produced in *E. coli* in inclusion body form and then solubilized and subjected to fast dilution to generate a refolded apo-enzyme. The protein was further purified in the presence of detergent by size-exclusion chromatography to generate the final protein sample used for crystallization trials. The Amzel laboratory in their structural study of *Z. mays* viviparous-14 expressed this CCD as a soluble, maltose-binding protein fusion in *E. coli* (Messing et al., 2010). Following metal-affinity chromatography and proteolytic removal of the N-terminal fusion tag, the liberated VP14 protein was purified by anion exchange and size-exclusion chromatography to generate a protein sample that was amenable to crystallization. Other investigators have employed *N*-terminal hexahistidine tags to allow purification of CCDs by immobilized metal affinity chromatography (Loewen et al., 2018; McAndrew et al., 2016). Finally, it was reported that co-expression of some CCDs with the prokaryotic chaperonin proteins GroEL and GroES promotes their folding and expression in soluble form rather than as inclusion bodies (Kuatsjah et al., 2019, 2021; Marasco & Schmidt-Dannert, 2008). In the case of RPE65, a natural source with relatively high expression of the protein allowed its purification from native RPE microsomal membranes by selective detergent extraction followed by anion exchange chromatography resulting in an RPE65 preparation that readily crystallized (Kiser, Golczak, Lodowski, Chance, & Palczewski, 2009).

As summarized in Fig. 2, our laboratory has taken a minimalist strategy for production and characterization of CCDs that involves expression of the native, untagged CCD in *E. coli* grown in standard LB media using the T7 promoter-based pET-3a expression plasmid as first described in (Sui et al., 2014). By using either low levels of inducing agents or omitting inducing agent and allowing expression to occur by leaky promoter activity, we have found that the CCDs from diverse families as well as point mutant variants of these enzymes can be expressed at high levels in soluble form allowing their two-step purification by classical biochemical methods (Daruwalla et al., 2020; Sui et al., 2014, 2015, 2017; Sui, Zhang, Golczak, Palczewski, & Kiser, 2016). Moreover, this system is readily adapted to expression in minimal media which allows for introduction of non-native metals into

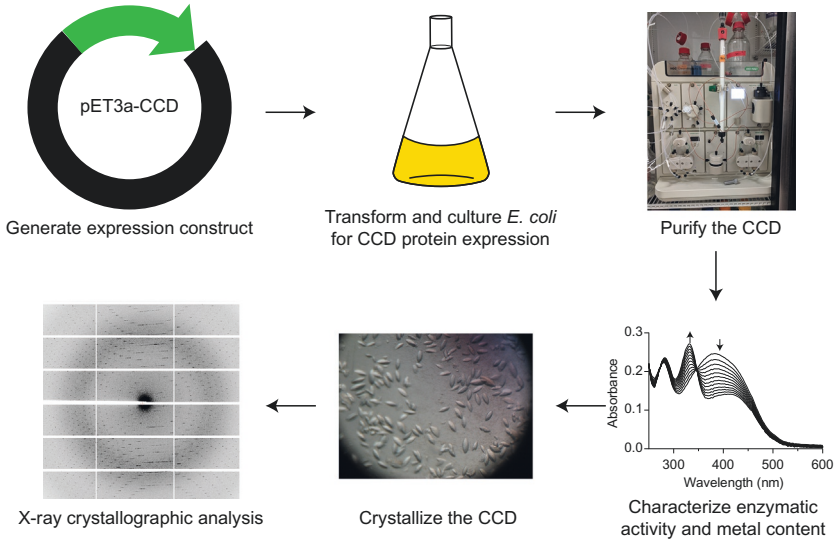

Fig. 2 An overview of protocol described in this work for the production of diffraction-quality CCD crystals. Each step is described in detail in the main text.

the active site that can assist in trapping unprocessed substrates for structural characterization (Daruwalla et al., 2020; Sui et al., 2017, 2018). This technique has been applied to three separate CCD enzymes from diverse clades allowing their successful crystallization and structure determination, which demonstrates the broad applicability of the method. In the text that follows, we provide details of these methods with the expectation that they can be successfully used for future CCD structure-function studies, potentially in combination with some of the other strategies described above.

3. Expression of native CCDs in *Escherichia coli* and their purification

3.1 Overview

Our CCD expression strategy starts with cloning the CCD coding sequence of interest into the pET3a expression vector, typically using the *Nde*I and BamHI cloning sites. Frequently, the coding sequence is obtained by customized gene synthesis, which allows its codon usage to be optimized for expression in *E. coli*. Following verification of the coding sequence by Sanger sequencing, the pET3a-CCD expression plasmid is transformed into T7 express *E. coli* competent cells and positive clones are selected on agar culture plates containing ampicillin. Positive clones are cultured in LB media

containing ampicillin at 37 °C and protein expression is accomplished through leaky T7 promoter activity during culturing of bacteria at lower temperatures of ~28 °C. Following lysis of the cells in a French pressure cell, the soluble protein is purified by a combination of ammonium sulfate fractionation or anion exchange chromatography, and gel filtration chromatography.

3.2 Equipment

- A 37 °C incubator
- A shaker-incubator capable of maintenance of the temperature between 28 and 37 °C
- A 42 °C water bath
- A suitable chromatography system for protein purification. Bio-Rad DuoFlow and NGC chromatography systems are used in our lab
- Spectrophotometer
- SDS-PAGE electrophoresis equipment
- Vortex
- French Pressure Cell
- Avanti JXN-26 centrifuge (Beckman) and appropriate rotor
- Optima XE-90 ultracentrifuge (Beckman) and appropriate rotor
- Optima MAX-TL ultracentrifuge (Beckman) and appropriate rotor

3.3 Reagents, cells, and other consumables

- 100 mg/mL ampicillin (Sigma-Aldrich, A0166-25g) stock solution prepared in ultrapure water
- Sterile LB media (Affymetrix/USB, C2566H) prepared in deionized water
- Freshly made LB/Agar (Fisher Scientific, BP-1423-500) plates prepared in deionized water and containing 100 mg/mL ampicillin
- Sterile SOC medium (Invitrogen,15544-034)
- T7 express *E. coli* competent cells (New England Biolabs, C2566H)
- Ammonium sulfate (Affymetrix/USB, 11254—5 kg)
- Buffer A: 10–20 mM HEPES-NaOH, pH 7 prepared in ultrapure water (Sigma-Aldrich, H3375 and S0899)
- Buffer B: 10–20 mM HEPES-NaOH, pH 7 containing 1 M NaCl (Sigma-Aldrich, S9888)
- 15 mL round bottom Falcon tubes (Corning, 352059)
- SDS-PAGE gels

- Coomassie blue R250 stain (Bio-Rad, 1610400)
- High-trap Q HP ion exchange column (GE Healthcare, 17-1154-01)
- Superdex 200 size-exclusion column (GE Healthcare, 28-9909-44)

3.4 Protocol

3.4.1 CCD expression

- Thaw one vial of T7 express cells on ice and transfer 50 μL of the cell suspension to an ice-chilled 15 mL round bottom Falcon tube. Add a 0.5–1 μL aliquot of the CCD plasmid DNA at a concentration of 20–80 ng/μL to the competent cells without mixing or other agitation followed by incubation on ice for 10 min
- Introduce the plasmid DNA into *E. coli* by heat shock at 42 °C for 30 s and then place the mixture back on ice for 2 min and supplement with 200 μL of SOC media. Place the cell suspension in a shaker incubator operating at ∼200 RPM and 37 °C for 1 h
- Plate variable volumes of the cell suspension (e.g., 1, 5, and 10 μL) on LB/ampicillin plates that have been pre-warmed to 37 °C to ensure that well-separated colonies are obtained. **NOTE**: In our experience, colonies selected from a dense lawn of bacteria exhibit relatively poor protein expression, hence the recommendation to aim for a plate sparsely populated with positive transformants.
- Incubate the LB/Ampicillin plates at 37 °C for ∼16 h (i.e., overnight) to allow growth of positive colonies
- Remove the plates from the incubator and pick ∼10 colonies using a sterile pipet tip and inoculate into a 15 mL round-bottom Falcon tube containing 3 mL of LB/Amp broth. **NOTE:** We find that protein expression is optimal when fresh colonies are used for the inoculation as opposed to colonies picked from plates that have been stored at 4 °C.
- Vortex the 3 mL starter culture for 10 s to help disperse the bacterial cell material and then place in a shaker-incubator operating at 225 RPM and 37 °C for 3 h. The starter culture should be moderately turbid at the end of this incubation period (e.g., $OD_{600nm} \sim 0.5$).
- Inoculate the starter culture into a 1 L of LB/Amp and place back into the shaker-incubator to grow until its OD_{600nm} reaches 0.4–0.6. At this time, adjust the incubation temperature to 28 °C and add an extra 100 mg of ampicillin to the culture. Allow the culture to incubate for ∼16 h (i.e., overnight)

- On the following day, collect the cells by centrifugation and then resuspend in 50 mL of 10–20 mM HEPES-NaOH, pH7 by vigorous vortexing. **NOTE:** At this point, the cell suspension can be used immediately or frozen at −80 °C for future use.
- For cell lysis, we find that the French Press is a reliable method for achieving complete cell disruption, although other methods such as nitrogen cavitation and sonication are also likely suitable. Lyse the cells and ultracentrifuge at 100,000 × *g* for 30 min to ensure that genuinely soluble CCD protein is used for downstream purification procedures

3.4.2 Native CCD purification methods

All purification methods are carried out on ice or at 4 °C unless otherwise noted. Once purified CCD is obtained using the methods described below or others, we concentrate the sample to at least 50 mg protein/mL in an appropriately buffered solution (typically 20 mM HEPES, pH7 with or without 200 mM NaCl), flash freeze it in liquid nitrogen, and then store it at −80 °C until needed for downstream use.

3.4.2.1 Ammonium sulfate fractionation

- We have used this method to purify *Syn*ACO, which does not bind to anion exchange resin under the conditions we have studied
- Add crystalline ammonium sulfate slowly to the supernatant fraction obtained from the *E. coli* lysate over the course of 30 min with constant gentle stirring to the desired percentage saturation (see Appendix A in (Scopes, 1994) for the relevant precipitation tables). Allow the mixture to continue stirring for an additional 30 min after the full quantity of ammonium sulfate has been added. **NOTE:** We have found that CCDs typically precipitate between 20% and 50% saturation
- Centrifuge the mixture at 46,000 × *g* for 20 min and remove the supernatant for analysis. Redissolve the pellet in ice-cold buffer A by gentle pipetting and subject the resulting mixture to ultracentrifugation at 100,000 *g* for 30 min. Collect the resulting supernatant and analyze along with unprecipitated material by SDS-PAGE

3.4.2.2 Anion exchange chromatography

- Most of the CCDs we have studied bind to anion exchange resin making this a generally useful purification technique. Protein purification is conducted on one of a number of protein purification chromatography systems. We typically use prepacked High-trap Q anion exchange columns

for CCD purification experiments, although similar resins would also likely be suitable. In several cases we have studied, the CCD binds to this column weakly which necessitates the protein to be in as low ionic strength buffer as possible

- Prepare the column by a high salt wash with 3–5 column volumes of buffer B followed by re-equilibration with buffer A until the conductivity restabilizes
- Pump the supernatant through the column at a rate of 1–2 mL/min. Wash the column with buffer A until the conductivity stabilizes. Elute the bound proteins via a linear gradient from 0 to 0.5 M NaCl followed by a step increase to 1 M NaCl to release the most tightly associated proteins. Analyze the eluted fractions with significant A_{280} values for the protein of interest by SDS-PAGE. Once the initial elution profile of the CCD is known, the gradient can be optimized to achieve better separation from contaminants

3.4.2.3 Size-exclusion chromatography

- For all of the CCDs we express for crystallization experiments, size-exclusion chromatography is used to remove large protein aggregates and to allow an assessment of the monodispersity of the sample, which is an attribute frequently critical for successful protein crystallization. Depending on the scale of the protein sample we use either 120 mL or 25 mL Superdex 200 size-exclusion columns. Protein purification is conducted on one of a number of protein purification chromatography systems
- Ultracentrifuge the partially purified CCD obtained from either ammonium sulfate fractionation or anion exchange chromatography to remove any large aggregates and then load onto the appropriate column which has been equilibrated with one column volume of Buffer A or Buffer A containing 200 mM NaCl depending on the sensitivity of the protein under study to salt. Moderate salt conditions (~150–200 mM) block electrostatic interaction of proteins with the size-exclusion media and therefore are likely to give better estimates of the protein size, which can be approximated by comparison to standards. Finally, collect and analyze the eluted fractions with significant A_{280} values for the protein of interest by SDS-PAGE

3.5 Expected results

Example SDS-PAGE gels documenting the purification of *Syn*ACO and *Nd*CCD are shown in Figs. 3 and 4. It is difficult to predict whether a

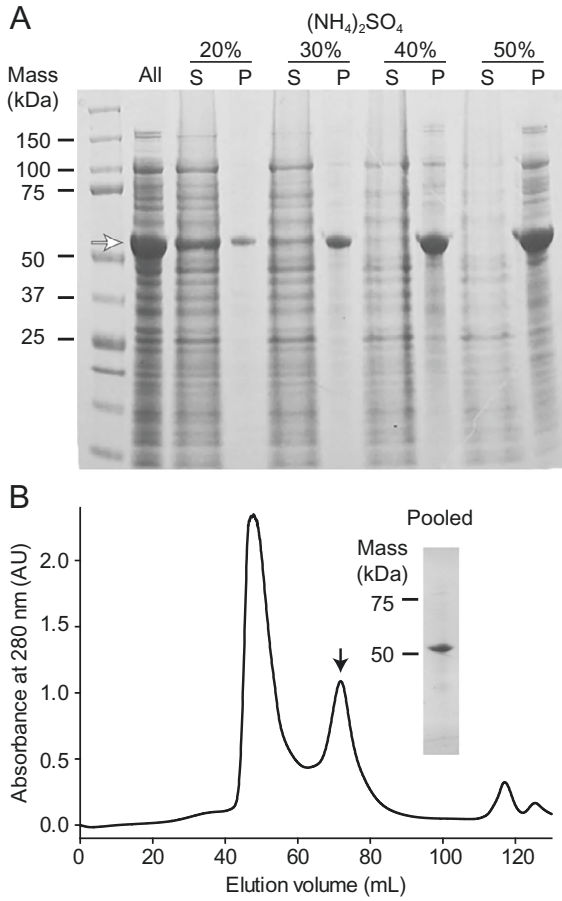

Fig. 3 Purification of SynACO from *E. coli* supernatant by ammonium sulfate fractionation and size-exclusion chromatography. (A) Coomassie-stained SDS-PAGE gel showing the step-wise precipitation of *Syn*ACO (band indicated by a white arrow) with increasing concentrations of ammonium sulfate. (B) Chromatogram showing the elution of *Syn*ACO obtained from the 40% saturation pellet in panel A from a 120 mL Superdex 200 size-exclusion column. The peak indicated by arrow represents monomeric *Syn*ACO while the large peak at the front of the column is aggregated material. The inset shows a Coomassie-stained SDS-PAGE gel of the pooled fractions from size-exclusion chromatography. *This figure is reused with permission from Sui, X., Kiser, P. D., Che, T., Carey, P. R., Golczak, M., Shi, W., et al. (2014). Analysis of carotenoid isomerase activity in a prototypical carotenoid cleavage enzyme, apocarotenoid oxygenase (ACO).* Journal of Biological Chemistry, 289*(18), 12286–12299.*

CCD of interest will express in soluble form in this expression system. Therefore, the safest approach is to test a variety of sequences of interest with a moderate degree of sequence variability. As noted above, CCD expression in inclusion bodies can sometimes be converted to soluble expression by

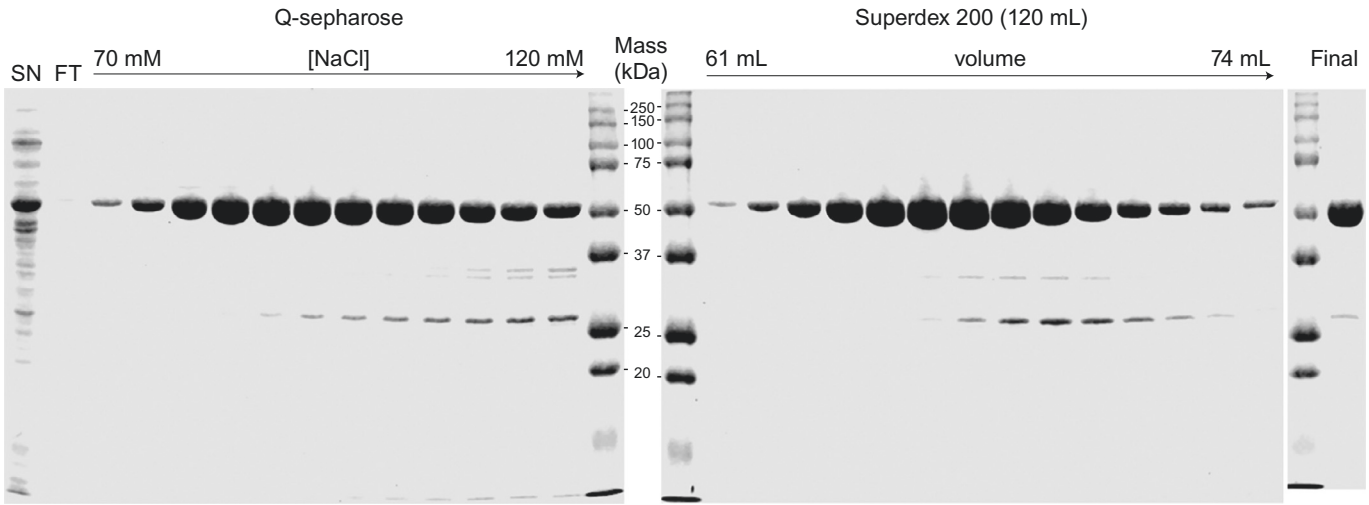

Fig. 4 Purification of NdCCD from E. coli supernatant by ion exchange and size-exclusion chromatography. The left-most gel shows the starting supernatant (SN) loaded onto the High-trap Q HP column, the flow-through (FT), and fractions eluted by a linear gradient of NaCl. The NdCCD band migrates just above the 50 kDa molecular weight marker. The fractions shown were pooled, concentrated, and applied to a 120 mL Superdex 200 column. Eluted fractions from this column are shown in the middle gel. The final concentrated sample is shown in the rightmost gel. A minor impurity is seen just above the 25 kDa molecular weight marker. *This figure is reused with permission from Daruwalla, A., Zhang, J., Lee, H. J., Khadka, N., Farquhar, E. R., Shi, W., et al. (2020). Structural basis for carotenoid cleavage by an archaeal carotenoid dioxygenase.* Proceedings of the National Academy of Sciences of the United States of America, 117*(33), 19914–19925.*

co-expression of chaperone proteins. In terms of protein purification, we first attempt anion exchange chromatography as an initial purification step for a given CCD. As stated above, the CCDs we have studied to date often bind to anion exchange media weakly, which necessitates that these enzymes be in low ionic strength conditions during passage over the media. If the enzyme fails to bind to the column, the anion exchange step can still serve as a purification step by removing many *E. coli* proteins that bind to anion exchange resin from the flow-through. This flow-through can then be used for ammonium sulfate fractionation experiments. All CCDs we have studied to date can be precipitated with ammonium sulfate with retention of enzymatic activity. The ability to greatly concentrate CCDs by precipitation makes this a useful procedure to prepare samples for size-exclusion chromatography, which necessitates the samples be in a volume no more than 3% of the column volume. Following ammonium sulfate fractionation, a portion of the *Syn*ACO is typically observed to elute in the void volume of the column. This fraction represents aggregated and catalytically inactive material. From a 120 mL Superdex 200 column, the active *Syn*ACO protein elutes at ~73 mL, which corresponds to a mass intermediate between the monomer and dimer.

If the purity is not sufficient, higher resolution ion exchange resin can be used, such as MonoQ-type columns. Of note, a sample judged completely pure based on SDS-PAGE is not necessary for CCD crystallization in the cases we have studied. However, use of insufficiently pure samples for crystallization trials may affect crystal quality and increase the risk of crystallizing contaminants.

4. Spectrophotometric assay of CCD activity

4.1 Overview

During the process of CCD purification, it is important to determine whether the protein retains its catalytic function and if the purification step improves the specific activity of the sample. For newly studied CCDs, it is critical to first evaluate the substrate specificity and regioselectivity of the enzyme, which are most readily evaluated by high-performance liquid chromatography and mass spectrometry. These methods have been described in detail previously and will not be repeated in this article (Thomas, Ramkumar, & von Lintig, 2020). Once a suitable substrate is known, the activity of the enzyme can be assessed in a straightforward manner by UV/Vis spectroscopy by monitoring either the rate of substrate consumption

or of product appearance (Sui et al., 2016, 2018). Alternatively, activity can be monitored by following the consumption of O_2 after addition of the organic substrate as previously reported (Kuatsjah et al., 2019, 2021). Below, we describe the procedure we use to measure cleavage of all-*trans*-beta-apo-8′-carotenol by *Syn*ACO. Because apocarotenoids are lipophilic molecules, detergents are needed to keep them in solution and help deliver them to the enzyme active site. Notably, certain linear detergents (e.g., tetraoxyethylene octyl ether) strongly inhibit CCD activity (Sui et al., 2014) and should be avoided for such assays. We have found that Triton X-100 at a concentration of 0.05% v/v is suitable for the study of apocarotenoid cleaving enzymes (Sui et al., 2014). Other detergents such as n-octyl beta-D-thioglucopyranoside (OTG) and lauryl maltose neopentyl glycol (LMNG) are ideal for measurement of carotenoid cleavage (Thomas et al., 2020). Notably, detergents are not necessary for assays of SCO activity. Finally, a reducing agent such as tris(2-carboxyethyl)phosphine (TCEP) or ascorbic acid can be included to enhance enzymatic activity by helping maintain the iron center in the ferrous oxidation state (Schwartz et al., 1997; Sui et al., 2015). For more details about the considerations surrounding the accurate measurement of steady-state kinetic parameters, the reader is referred to one of the many detailed enzymology texts (e.g., Copeland, 2000).

4.2 Equipment

- A suitable UV/Vis spectrophotometer. We use a Perkin-Elmer Lambda Bio + for routine measurements

4.3 Reagents

- Buffer A containing 1 mM tris(2-carboxyethyl)phosphine (TCEP, Sigma-Aldrich, 646,547) and 0.05% v/v Triton X-100 (Sigma-Aldrich, X100–500 mL) (Assay buffer)
- 100 mM stock solution of all-*trans*-beta-apo-8′-carotenol (Sigma-Aldrich, 10,810) in 100% ethanol prepared as described in (Sui et al., 2014).

4.4 Other materials

- A suitable micro or semi-micro quartz cuvette (e.g., Hellma Analytics, 105-202-15-40)

4.5 Protocol

- Add a suitable volume of *Syn*ACO-containing sample or 2–4 μg of purified *Syn*ACO to 200 μL of assay buffer. Incubate for 5 min and then add all-*trans*-beta-apo-8′-carotenol substrate to a final concentration of 150 μM to initiate the reaction. Alternatively, steady-state kinetic parameters can be determined using a range of substrate concentrations. Monitor the progress of reaction by measuring the change in substrate absorbance at 424 nm over time
- Convert the absorbance change into the rate of substrate consumption using a standard curve. Use an enzyme omitted reaction control to determine the rate of non-enzymatic loss of the substrate

4.6 Expected results

An effective purification protocol should generate protein samples with progressively increased specific activity. As shown in (Sui et al., 2014) for *Syn*ACO, starting from a specific activity of 0.02 units/mg in the crude supernatant, the specific activity was increased ~24-fold after ammonium sulfate fractionation and gel filtration chromatography with high recovery of the total activity (~72%). *Syn*ACO has reported k_{cat} and K_m values of $0.21\,s^{-1}$ and 47 μM, respectively, towards all-*trans*-beta-apo-8′-carotenol (Sui et al., 2014). SCOs typically exhibit higher turnover numbers as compared to carotenoid-cleaving CCDs, likely owing to the greater aqueous solubility of SCO substrates and products (Kiser, 2019).

5. Production of metal-substituted CCDs

5.1 Overview

The production of metal-free or metal-substituted CCDs is achieved by expressing the protein in M9 minimal media. Under the nutrient-limited growth condition, the target divalent metals are exogenously supplemented in the media for potential incorporation into the CCD metal-binding site during protein expression. Therefore, it is essential to avoid metal contamination during CCD expression, especially iron which is present ubiquitously in the environment (Frey & Reed, 2012). In our system, this was achieved by choosing the target metal salt with highest purity and using extensively cleaned glassware for protein production. Efforts are also required to minimize metal contamination during protein purification. In the final purified CCDs, the metal incorporation can be accessed by the

activity assay procedure described above, as the incorporated non-native divalent metal would render a decreased CCD activity compared to the native ferrous iron. For accurate determination, metal content can be measured by ICP-OES and TPTZ methods (see Section 6).

5.2 Equipment

- As listed above for the purification of native CCDs

5.3 Chemicals

- All solutions described below are prepared in ultrapure (18.2 MΩ-cm) water
- 5 × M9 salts: 64 g Na_2HPO_4-$7H_2O$ (Sigma-Aldrich, 431,478), 15 g KH_2PO_4 (Sigma-Aldrich, 229,806), 2.5 g NaCl, 5 g, NH_4Cl (Sigma-Aldrich, 254,134) dissolved in ultrapure water to a final volume of 1 L and autoclaved
- M9 minimal media: 600 mL of ultrapure water, 100 μL of sterile filtered 1 M $CaCl_2$ (Fisher Scientific, C79–500), 200 mL of 5 × M9 salts, 2 mL of sterile-filtered 1 M $MgSO_4$ (Fisher Scientific, BP213-1), 20 mL of sterile-filtered 20% w/v glucose (Fisher Scientific, D16-500), 16 mL of 50% v/v glycerol (Fisher Scientific, BP229–4), *quantum sufficit* ultrapure water to make 1 L final volume
- Divalent metal salts, $CoCl_2 \cdot 6H_2O$ (Sigma-Aldrich, 60,820), $MnCl_2 \cdot 4H_2O$ (Sigma-Aldrich, 203,734), $CuCl_2 \cdot 2H_2O$ (Sigma-Aldrich, 307,483), $(NH_4)_2Fe(SO_4)_2 \cdot 6H_2O$ (Mohr's salt, Sigma-Aldrich, 215,406)
- 1 M isopropyl β-D-1-thiogalactopyranoside (IPTG, Anatrace, I1003)
- 5 mM ethylenediaminetetraacetic acid, pH 8 (EDTA, Alfa Aesar, A1071336)
- All other chemical reagents are used as for native CCD enzymes

5.4 Protocol

- Transform the pET3a vector harboring target CCD into the T7 express BL21 *E. coli* strain, and plate the cells on a LB agar plate containing 100 μg/mL ampicillin
- After overnight growth at 37 °C, inoculate several fresh *E. coli* colonies into 2 mL of LB media containing 100 μg/mL ampicillin, and allow it to grow for ~5 h at 37 °C in a shaker-incubator
- Collect the cells by centrifugation at 3220 × *g* for 15 min at 37 °C and remove the LB media

- Resuspend the cell pellet in 1 mL of M9 minimal media and transfer the cell suspension into 1000 mL of M9 minimal media containing 100 μg/mL ampicillin
- Continue the growth at 37 °C at 235 RPM until the density reaches ~0.5 at OD_{600nm}
- Decrease the temperature to 28 °C and supplement the 1000 mL culture with 30 mg of target divalent metal salts for the production of metal-substituted CCDs. Metal-free CCDs (apo-CCDs) can also be produced by omitting the addition of divalent metals
- At the same time, induce protein production by adding IPTG to a final concentration of 100 μM and supplement the culture with an additional 100 μg/mL ampicillin
- After overnight protein production at 28 °C, harvest the cells by centrifugation, resuspend in Buffer A, and store the cell pellet at −80 °C
- To purify apo- or metal-substituted CCDs, follow the protocol outlined above for the native CCD enzyme taking care to avoid metal contamination. It is recommended to thoroughly wash the chromatography columns and tubing with 5 mM EDTA, pH 8 solution to help remove contaminating divalent cations

5.5 Expected results

Owing to the nutrient-restricted nature of M9 media, the total yield of bacterial cell pellet and overall protein expression is typically lower than that achieved with LB media. Because the M9 media contains glucose, a suppressor of L8-UV5 lac promoter activity (Pan & Malcolm, 2000), the addition of IPTG may be required to stimulate adequate levels of recombinant protein expression. Based on past experience with *Syn*ACO, we have found that apo enzyme is readily produced by this method indicating that a metal ion is not required for protein folding in vivo. Of the various non-native metals we have tested, Co^{2+} is most reliably incorporated into the CCD active site. In concentrated form, Co-substituted CCDs exhibit a color (described as pale pink, bronze or purple depending on the CCD) differing from that of the native Fe-bound enzyme, which arises from *d-d* optical absorbance bands in the 400–600 nm range (Table 1). Despite its positive impact on cell growth, Mn^{2+} was not effectively incorporated into the active site of *Syn*ACO. The M9 media expression method can also be used to produce CCDs enriched in ^{57}Fe for use in spectroscopic studies (Sui et al., 2017).

Table 1 Optical absorbance peaks of co-substituted CCDs.

CCD protein	Optical absorbance bands (nm)	References
*Syn*ACO	429, 555, 584	Sui et al. (2018)
*Nd*CCD	428, 524, 562	Daruwalla et al. (2020)
LSD4	460, ~525, 570	Kuatsjah et al. (2021)

6. Quantification of CCD metal content

6.1 Overview

The inductively coupled plasma optical emission spectroscopy (ICP-OES) analysis is performed to quantify the metals associated with purified CCD enzymes. This method uses the optical emission spectra characteristic of a given element to quantify the elemental abundance based on spectral intensities. It has the advantage of being able to simultaneously determine the abundance of multiple elements of interest in the sample, for example all first-row transition metals. Prior to this assay, the bound metal ions in CCDs are extracted by denaturation of purified proteins in nitric acid solution.

TPTZ (2,4,6-Tripyirdyl-*s*-triazine) is used as a colorimetric reagent for detecting iron. It binds ferrous iron resulting in the formation of a violet colored, water-soluble compound (Fig. 5). The addition of hydroxylamine to the assay system will reduce any Fe(III) in the sample to Fe(II). This rapid and inexpensive assay is useful for quantifying the amount of iron in CCD preparations obtained from normal growth media.

For determination of the iron/CCD stoichiometry, it is critical that the CCD concentration in the sample be accurately determined. Protein concentration estimates made by A_{280} readings or Bradford assays using a standard protein such as bovine serum albumin are often not accurate for CCDs due to their differing extinction coefficients or capacity for inducing color change, respectively. Absolute amino acid quantification of purified and hydrolyzed CCD samples allows an accurate value for the extinction coefficient of native CCD in solution to be determined. We typically submit samples for amino acid analysis to the Protein Chemistry Laboratory at Texas A&M University.

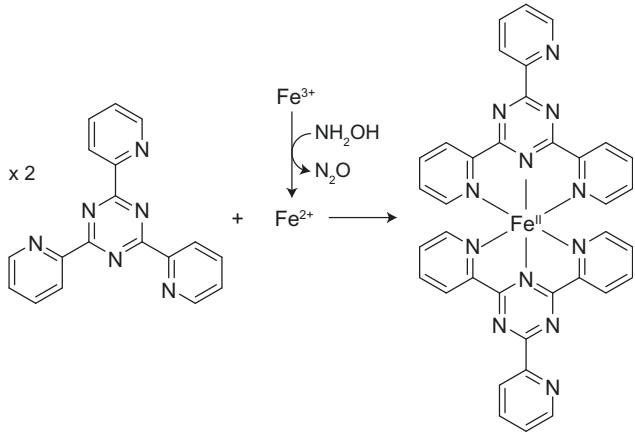

Fig. 5 The chemical basis of the TPTZ assay for ferrous iron. Two molecules of TPTZ react with divalent iron to form a 6-coordinate complex with an optical absorbance band at ~596 nm. Any ferric iron in the sample can be converted to Fe^{2+} by addition of hydroxylamine to the assay system.

6.2 Method

6.2.1 ICP-OES method

6.2.1.1 Equipment

- Bench-top rocker (VWR, 3451681)

6.2.1.2 Consumables

- 0.22 μm membrane filter (Millipore, SLGP033RS)
- 10 mL plastic syringe (Becton Dickinson, 305,482)
- 70% nitric acid solution (Sigma-Aldrich, 225,711)
- Ultrapure water

6.2.1.3 Protocol

- Place a known amount of purified CCDs (native or metal-substituted) in 5–10 mL 1% v/v nitric acid solution to hydrolyze the protein and liberate the protein-bound metals. The protein typically forms a white aggregate upon addition to the nitric acid solution. In general, we aim for a final expected concentration of 1 part per million (ppm) for the metal of interest. For CCDs, this corresponds to approximately 5 mg of purified protein per 5 mL of the nitric acid solution

- Perform the digestion for 3 h at room temperature with rocking on a bench-top rocker
- Remove the protein precipitates by filtering the mixture through a 0.22 μm membrane and collect the filtrate
- Perform the same digestion in step 1–3 with only the protein buffer solution as a control for the background metal content
- Submit the solutions thus obtained for ICP-OES analysis. We typically use the ICP-OES service provided by the Soil Research Analytical Laboratory at the University of Minnesota
- Determine the molar extinction coefficient of the purified CCD by amino acid quantification and calculate the molar amount of protein to be used to prepare samples for ICP-OES analysis
- Calculate the CCD-metal stoichiometry based on ICP-OES results

6.2.2 TPTZ method

6.2.2.1 Equipment

- Thermomixer (VWR)
- Table-top microcentrifuge (Eppendorf)
- UV-Cuvette micro (PerkinElmer)
- UV/visible spectrophotometer (PerkinElmer)

6.2.2.2 Chemicals

- All reagents and samples are prepared in ultrapure water
- 2 N HCl (Sigma-Aldrich, 320331)
- 10 mM 2,4,6-tri(2-pyridyl)-*s*-triazine (Sigma-Aldrich, 93285) in 0.2 N HCl
- 20% *w*/*v* trichloroacetic acid (Sigma-Aldrich, T6399)
- 3 M sodium acetate (Sigma-Aldrich, 241245)
- 20 mM Hydroxylamine-HCl, pH 6 (Sigma-Aldrich, 379921)
- 100 μM Mohr's salt (Sigma-Aldrich, 215406)

6.2.2.3 Protocol

- **NOTE:** if the protein sample quantity is limiting, the following protocol volumes can be scaled down 10-fold and the final sample read using a micro-volume cuvette
- Step 1: Prepare 200 μL samples of the CCD at a concentration of 100 μM. We typically prepare two sets of samples, one for analysis in the presence of hydroxylamine and another in its absence. Additionally,

a 200 μL sample of 100 μM Mohr's salt as well as a sample of the protein buffer alone should be prepared for use as a standard and blank, respectively. Samples should be prepared in triplicate to assess variability

- Step 2: Add 250 μL of 20% trichloroacetic acid, 250 μL of 2 N HCl, and 300 μL of ultrapure water to each sample tube and mix by vortexing
- Step 3: Heat the samples at 95 °C for 15 min and then centrifuge them in a microcentrifuge to pellet precipitated protein
- Step 4: For each sample to be analyzed, prepare a 300 μL reaction mixture consisting of 30 μL of 10 mM TPTZ, 264 μL of 3.0 M sodium acetate and 6 μL of 20 mM of hydroxylamine (6 μL of ultrapure water for reactions without hydroxylamine) in separate microcentrifuge tubes
- Step 5: Add 750 μL of supernatant from Step 3 to the reaction mixture from Step 4, incubate the mixture at ambient temperature for 30 min, and then centrifuge the sample in a microcentrifuge to remove any particulates
- Step 6: Transfer an appropriate volume of the final sample to a clean cuvette and record its absorbance at 596 nm
- Use the absorption measurements from the Mohr's salt reactions carried out in the presence of hydroxylamine to calculate the molar absorptivity (ε) by application of the Beer-Lambert equation: $\varepsilon = A/(c \cdot l)$, where A is the absorbance at 596 nm, l, length of the light path and c is the iron concentration
- Use this molar absorptivity, which should be around 22.6 mM^{-1} cm^{-1}, to calculate the final iron concentration in the samples accounting for all dilution factors. The reactions carried out in the presence of hydroxylamine report the total iron concentration while those determined in its absence report only the ferrous iron in the sample

6.3 Expected results

It is typical for CCDs expressed using the protocol described in Section 3 to exhibit an iron to CCD stoichiometry of 70–100%. Occasionally, the stoichiometry can exceed 100% which indicates the presence of adventitious iron in the sample. If adventitious iron is problematic for a given experiment, it may be possible to remove it by additional steps of protein purification. If significantly substoichiometric iron concentrations are observed, it may be possible to boost the level of metal loading by addition of iron to the

expression culture. Iron is typically the major first row transition metal found in CCD samples obtained from LB growth media. There can occasionally be significant amounts of zinc in the sample as well, although this is unlikely to be bound to the active site based on anomalous diffraction analyses.

ICP-OES analysis is ideal to measure the metal content of samples prepared as described in Section 5. This technique confirms that it is possible to generate apo-CCD samples by omitting first row transition metals from the culture medium. Additionally, it allows the level of iron contamination in samples produced in the presence of cobalt to be accurately determined. We have observed that cobalt can be incorporated into CCDs at near stoichiometric levels. However, all Co-CCD samples we have analyzed to date contain some amount of contaminating iron. In some cases, the low level of iron does not interfere with the goal of obtaining a stable CCD-substrate complex for structural analysis. However, in another case we observed that carotenoid substrate was oxidatively cleaved during the purification and crystallization process despite a bulk of the enzyme being in the cobalt-bound state. Great care should be exercised to minimize the potential for iron incorporation in the sample.

7. Crystallization of CCDs (with and without ligands)

7.1 Overview

The crystallization of CCDs can be accomplished via standard vapor-diffusion methodology by employing commercially available sparse matrix screening kits. As with any new crystallization project, the conditions under which the CCD of interest will crystallize cannot be predicted a priori and it is wise to test a variety of different conditions. Besides the crystallization solution itself, other potentially important variables include the crystal trial configuration (i.e., hanging vs. sitting drop), preparation and incubation temperatures, protein concentration and the composition of the solution in which it is contained. Another critical variable is the choice of detergent used for CCD purification and crystallization. Generally, we test up to 300–400 distinct crystallization conditions for a given purified protein with trays set up at room temperature and incubated at both 8 and 20 °C.

To elucidate the active site determinants, substrate specificity, and cleavage activity, the structure of a native ligand-bound CCD complex becomes necessary. Structural characterization of many members of this class over the last several years has made it possible to observe the diverse yet specialized

substrate-binding clefts of each of these proteins. Recent studies have shown that substitution of native iron in the active site with cobalt enables the stable binding of substrate ligands in the active site for structural characterization. However, the success of such a strategy depends on the near complete elimination of iron-bound protein from the sample as even low levels can lead to consumption of substrate over the course of the crystallization experiment. Below we describe the successful co-crystallization of Co-CAO1 in complex with piceatannol.

7.2 Equipment

- UV/visible spectrophotometer (PerkinElmer)
- Refrigerator incubators (8 and 22 °C)
- Leica stereoscopic microscope

7.3 Chemicals and other consumables

- Consumables for SDS-PAGE
- HEPES buffer (Sigma-Aldrich)
- Triton X-100 (Sigma-Aldrich)
- Amicon Ultra-4 Centrifugal Filters (30 kDa MW cutoff) (Merck Millipore, UFC903024)
- Piceatannol (TCI, P1928)
- MidasPlus crystallization screen (Molecular Dimensions, MD1-106)
- Sodium polyacrylate 2100 (Aldrich, 420344)
- Dimethyl sulfoxide (DMSO) (Sigma Aldrich, D128-1)
- Xylitol (Acros Organics, 225985000)
- Glycerol (Fisher Scientific, BP229-4)
- 24-well, pre-greased crystallization trays (Hampton Research, HR3-170)
- Siliconized Cover Slides Thick Squares (22 mm) (Hampton Research, HR3-225)
- Crystal Loops (e.g., Mitegen, M5-L18SP-200)

7.4 Protocol

7.4.1 General CCD crystallization protocol

- Prepare a 10–40 mg/mL solution of the CCD of interest in 10 mM HEPES-NaOH or another suitable minimal buffer system

- Pipette 0.5 mL of crystallization cocktail solutions (from a commercial sparse matrix screen or homemade) into each well of a 24-well pre-greased crystallization plate
- Mix the purified protein sample with the crystallization cocktail in a 1:1 ratio on a siliconized coverslip, invert the coverslip, place over the remaining crystallization cocktail, and seal the chamber. Take care to avoid introducing air bubbles into the drop during pipetting
- After completing set up of the crystallization tray, carefully transfer the plate into an incubator. Take care to avoid bumping or otherwise perturbing the tray
- Observe each crystallization trial under an appropriate microscope after 1–2 days of incubation paying close attention to the presence of crystalline material in the drop. The drops should be re-inspected periodically as crystals can take weeks or even months to form in some cases
- The identity of any observed crystals can be checked by looping the crystal, washing it in crystallization solution, and then dissolving it in water for SDS-PAGE analysis. Protein crystals are normally relatively fragile and will typically quickly dissolve in pure water
- The goal is to obtain relatively large single crystals for X-ray diffraction analysis. Frequently, the initial crystals obtained can be further optimized by changing the variables described above. For further details, the reader is referred to a classic textbook on macromolecular crystallization (McPherson, 1999).
- Prior to harvesting of optimized crystals for X-ray diffraction analysis, it must be ensured that a sufficient level of cryoprotectant be present in the crystal-containing solution in order to suppress the formation of ice, which can adversely impact the X-ray diffraction pattern due to the occurrence of ice rings as well as distortion of the crystalline structure. A variety of agents can be used as cryo-protectants. For CCD crystals, we typically use glycerol or xylitol solutions which can be included during crystal growth or provided in a soaking solution that the crystal is placed in for a given period of time prior to it being looped and flash frozen

7.4.2 Crystallization of Co-CAO1 with piceatannol

- Pipette 0.5 mL solution of the crystallization cocktail solution containing 42–43% sodium polyacrylate 2100 and 0.1 M HEPES-NaOH, pH 6.5 into each well of a 24-well crystallization plate

- Mix 20 mg/mL purified cobalt-substituted CAO1 enzyme with the crystallization solution in a 1:1 ratio on a siliconized cover slide and set up for crystallization by the hanging vapor diffusion method in the 24-well plate
- Incubate the plates at 8 °C
- Monitor for crystals (usually rod-shaped and hexagonal in cross section) over the next few days
- Harvest these crystals over the following 1–2 weeks using appropriate crystal loops
- To obtain a complex between Co-CAO1 and piceatannol, add the ligand dissolved in DMSO to the purified protein sample to achieve a final piceatannol concentration of 3 mM
- Centrifuge samples at 71,680 × *g* for 15 min to pellet any aggregates before setting up crystals using the same conditions as above
- To ensure full occupancy of the ligand, the crystals can additionally be soaked overnight in the crystallization solution containing 10 mM of the ligand prior to harvesting
- Harvest the crystals in microloops and store them in liquid nitrogen or liquid nitrogen vapor until X-ray data collection

7.5 Expected results

Fig. 6 presents optimized crystals of CCDs obtained using the methods described in this protocol. If a well-expressing CCD can be obtained in pure form and at a sufficient concentration, there is a reasonable chance that the protein will be amenable to crystallization. Nevertheless, there is never a guarantee of success as we have experienced with certain CCDs that can be obtained in large quantities in purified, active form but are highly recalcitrant to crystallization. For this reason, if a protein fails to crystallize after a three or four hundred trials (i.e., 300–400 distinct and diverse conditions), it is probably advisable to alter the construct in some way (e.g., trimming of flexible regions or surface entropy reduction; Derewenda & Vekilov, 2006, via site-directed mutagenesis) or to switch to a different homolog with the same activity of interest. The cobalt substitution method has been successful in trapping substrates in the active site for structural characterization. However, the presence of even a minor fraction of iron-bound enzyme can generate enough activity to turn over substrate added during purification (Daruwalla et al., 2020; Kuatsjah et al., 2021). As such, it is imperative to take all necessary steps to avoid introducing iron into the sample, which could occur at any point due to the ubiquitous presence of iron in the environment.

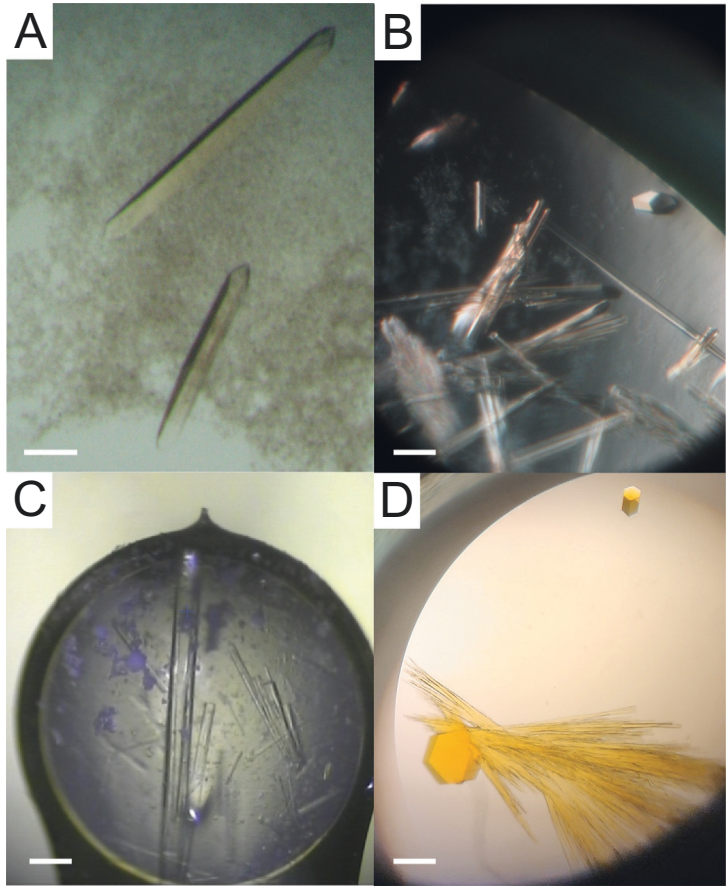

Fig. 6 CCD crystals obtained using the protocol described in this work. (A) Obelisk-shaped orthorhombic *Syn*ACO crystals in space group $P2_12_12_1$. (B) Trigonal CAO1 crystals in space group $P3_121$. (C) Hexagonal *Nd*CCD crystals in space group $P6_1$. (D) *Nd*CCD crystals in the same form shown in panel (C), but grown from protein purified in the presence of apocarotenoid substrate. Note their marked orange color. The scale bars in each panel represent approximately 100 μm. *Panel D is reused with permission from Daruwalla, A., Zhang, J., Lee, H. J., Khadka, N., Farquhar, E. R., Shi, W., et al. (2020). Structural basis for carotenoid cleavage by an archaeal carotenoid dioxygenase.* Proceedings of the National Academy of Sciences of the United States of America, 117*(33), 19914–19925.*

8. Summary

CCDs perform numerous important functions in nature and are responsible for generation of products of considerable economic valuable. High resolution structures of these proteins determined by X-ray

crystallography provide key insights into their catalytic activity. Such structures also open the door to rational mutagenesis approaches to alter substrate specificity or product formation, which could prove to be fruitful in generating rare carotenoid or stilbenoid compounds that are difficult to obtain through traditional synthetic chemistry approaches (Liang et al., 2021). Additionally, high resolution structural information can facilitate design of small molecule compounds to modulate the activity of CCDs for medical or agricultural purposes. It is our hope that the methods we have outlined in this chapter will facilitate such investigations.

Acknowledgments

We thank Dr. Johannes von Lintig (Case Western Reserve University) for valuable comments on this manuscript. This work was supported by funding from the Department of Veterans Affairs (I01BX004939), the National Science Foundation (CHE-2107713), the National Institutes of Health (R24EY027283), and an unrestricted grant from Research to Prevent Blindness to the Department of Ophthalmology at UC Irvine. The views expressed in this article are those of the authors and do not necessarily reflect the position or policy of the funding bodies or the United States government. The authors declare no competing financial interests.

References

Auldridge, M. E., Block, A., Vogel, J. T., Dabney-Smith, C., Mila, I., Bouzayen, M., et al. (2006). Characterization of three members of the Arabidopsis carotenoid cleavage dioxygenase family demonstrates the divergent roles of this multifunctional enzyme family. *Plant Journal*, *45*(6), 982–993.

Brefort, T., Scherzinger, D., Limon, M. C., Estrada, A. F., Trautmann, D., Mengel, C., et al. (2011). Cleavage of resveratrol in fungi: Characterization of the enzyme Rco1 from Ustilago maydis. *Fungal Genetics and Biology*, *48*(2), 132–143.

Bruno, M., Vermathen, M., Alder, A., Wust, F., Schaub, P., van der Steen, R., et al. (2017). Insights into the formation of carlactone from in-depth analysis of the CCD8-catalyzed reactions. *FEBS Letters*, *591*(5), 792–800.

Copeland, R. A. (2000). *Enzymes: A practical introduction to structure, mechanism, and data analysis* (2nd ed.). New York: Wiley.

Daruwalla, A., & Kiser, P. D. (2020). Structural and mechanistic aspects of carotenoid cleavage dioxygenases (CCDs). *Biochimica et Biophysica Acta, Molecular and Cell Biology of Lipids*, *1865*(11), 158590.

Daruwalla, A., Zhang, J., Lee, H. J., Khadka, N., Farquhar, E. R., Shi, W., et al. (2020). Structural basis for carotenoid cleavage by an archaeal carotenoid dioxygenase. *Proceedings of the National Academy of Sciences of the United States of America*, *117*(33), 19914–19925.

Derewenda, Z. S., & Vekilov, P. G. (2006). Entropy and surface engineering in protein crystallization. *Acta Crystallographica. Section D, Biological Crystallography*, *62*(Pt 1), 116–124.

Frey, P. A., & Reed, G. H. (2012). The ubiquity of iron. *ACS Chemical Biology*, *7*(9), 1477–1481.

Kamoda, S., & Saburi, Y. (1993). Cloning, expression, and sequence analysis of a lignostilbene-alpha,beta-dioxygenase gene from *Pseudomonas paucimobilis* TMY1009. *Bioscience, Biotechnology, and Biochemistry*, *57*(6), 926–930.

Kiser, P. D. (2019). Alkene-cleaving carotenoid cleavage dioxygenases. In R. A. Scott (Ed.), *Encyclopedia of inorganic and bioinorganic chemistry* John Wiley & Sons, Ltd.

Kiser, P. D., Golczak, M., Lodowski, D. T., Chance, M. R., & Palczewski, K. (2009). Crystal structure of native RPE65, the retinoid isomerase of the visual cycle. *Proceedings of the National Academy of Sciences of the United States of America*, *106*(41), 17325–17330.

Kiser, P. D., Lodowski, D. T., & Palczewski, K. (2007). Purification, crystallization and structure determination of native GroEL from Escherichia coli lacking bound potassium ions. *Acta Crystallographica Section F-Structural Biology Communications*, *63*(Pt 6), 457–461.

Kloer, D. P., Ruch, S., Al-Babili, S., Beyer, P., & Schulz, G. E. (2005). The structure of a retinal-forming carotenoid oxygenase. *Science*, *308*(5719), 267–269.

Kuatsjah, E., Chan, A. C. K., Katahira, R., Haugen, S. J., Beckham, G. T., Murphy, M. E. P., et al. (2021). Structural and functional analysis of lignostilbene dioxygenases from Sphingobium sp. SYK-6. *Journal of Biological Chemistry*, *296*, 100758.

Kuatsjah, E., Verstraete, M. M., Kobylarz, M. J., Liu, A. K. N., Murphy, M. E. P., & Eltis, L. D. (2019). Identification of functionally important residues and structural features in a bacterial lignostilbene dioxygenase. *Journal of Biological Chemistry*, *294*(35), 12911–12920.

Liang, N., Yao, M. D., Wang, Y., Liu, J., Feng, L., Wang, Z. M., et al. (2021). CsCCD2 access tunnel design for a broader substrate profile in crocetin production. *Journal of Agricultural and Food Chemistry*, *69*(39), 11626–11636.

Loewen, P. C., Switala, J., Wells, J. P., Huang, F., Zara, A. T., Allingham, J. S., et al. (2018). Structure and function of a lignostilbene-alpha,beta-dioxygenase orthologue from *Pseudomonas brassicacearum*. *BMC Biochemistry*, *19*(1), 8.

Marasco, E. K., & Schmidt-Dannert, C. (2008). Identification of bacterial carotenoid cleavage dioxygenase homologues that cleave the interphenyl alpha,beta double bond of stilbene derivatives via a monooxygenase reaction. *Chembiochem*, *9*(9), 1450–1461.

McAndrew, R. P., Sathitsuksanoh, N., Mbughuni, M. M., Heins, R. A., Pereira, J. H., George, A., et al. (2016). Structure and mechanism of NOV1, a resveratrol-cleaving dioxygenase. *Proceedings of the National Academy of Sciences of the United States of America*, *113*(50), 14324–14329.

McPherson, A. (1999). *Crystallization of biological macromolecules*. Cold Spring Harbor, NY: Cold Spring Harbor Laboratory Press.

Messing, S. A., Gabelli, S. B., Echeverria, I., Vogel, J. T., Guan, J. C., Tan, B. C., et al. (2010). Structural insights into maize viviparous14, a key enzyme in the biosynthesis of the phytohormone abscisic acid. *Plant Cell*, *22*(9), 2970–2980.

Moiseyev, G., Takahashi, Y., Chen, Y., Gentleman, S., Redmond, T. M., Crouch, R. K., et al. (2006). RPE65 is an iron(II)-dependent isomerohydrolase in the retinoid visual cycle. *Journal of Biological Chemistry*, *281*(5), 2835–2840.

Neidig, M. L., & Solomon, E. I. (2005). Structure-function correlations in oxygen activating non-heme iron enzymes. *Chemical Communications*, *47*, 5843–5863.

Oberhauser, V., Voolstra, O., Bangert, A., von Lintig, J., & Vogt, K. (2008). NinaB combines carotenoid oxygenase and retinoid isomerase activity in a single polypeptide. *Proceedings of the National Academy of Sciences of the United States of America*, *105*(48), 19000–19005.

Pan, S. H., & Malcolm, B. A. (2000). Reduced background expression and improved plasmid stability with pET vectors in BL21 (DE3). *BioTechniques*, *29*(6), 1234–1238.

Prado-Cabrero, A., Scherzinger, D., Avalos, J., & Al-Babili, S. (2007). Retinal biosynthesis in fungi: Characterization of the carotenoid oxygenase CarX from Fusarium fujikuroi. *Eukaryotic Cell*, *6*(4), 650–657.

Redmond, T. M., Poliakov, E., Yu, S., Tsai, J. Y., Lu, Z., & Gentleman, S. (2005). Mutation of key residues of RPE65 abolishes its enzymatic role as isomerohydrolase in the visual cycle. *Proceedings of the National Academy of Sciences of the United States of America*, *102*(38), 13658–13663.

Ruch, S., Beyer, P., Ernst, H., & Al-Babili, S. (2005). Retinal biosynthesis in Eubacteria: In vitro characterization of a novel carotenoid oxygenase from Synechocystis sp. PCC 6803. *Molecular Microbiology*, *55*(4), 1015–1024.

Schwartz, S. H., Tan, B. C., Gage, D. A., Zeevaart, J. A., & McCarty, D. R. (1997). Specific oxidative cleavage of carotenoids by VP14 of maize. *Science*, *276*(5320), 1872–1874.

Scopes, R. K. (1994). *Protein purification: Principles and practice* (3rd ed.). New York: Springer-Verlag.

Sui, X., Farquhar, E. R., Hill, H. E., von Lintig, J., Shi, W., & Kiser, P. D. (2018). Preparation and characterization of metal-substituted carotenoid cleavage oxygenases. *Journal of Biological Inorganic Chemistry*, *23*(6), 887–901.

Sui, X., Golczak, M., Zhang, J., Kleinberg, K. A., von Lintig, J., Palczewski, K., et al. (2015). Utilization of dioxygen by carotenoid cleavage oxygenases. *Journal of Biological Chemistry*, *290*(51), 30212–30223.

Sui, X., Kiser, P. D., Che, T., Carey, P. R., Golczak, M., Shi, W., et al. (2014). Analysis of carotenoid isomerase activity in a prototypical carotenoid cleavage enzyme, apo-carotenoid oxygenase (ACO). *Journal of Biological Chemistry*, *289*(18), 12286–12299.

Sui, X., Weitz, A. C., Farquhar, E. R., Badiee, M., Banerjee, S., von Lintig, J., et al. (2017). Structure and spectroscopy of alkene-cleaving dioxygenases containing an atypically coordinated non-heme iron center. *Biochemistry*, *56*(22), 2836–2852.

Sui, X., Zhang, J., Golczak, M., Palczewski, K., & Kiser, P. D. (2016). Key residues for catalytic function and metal coordination in a carotenoid cleavage dioxygenase. *Journal of Biological Chemistry*, *291*(37), 19401–19412.

Thomas, L. D., Ramkumar, S., & von Lintig, J. (2020). Expression and characterization of mammalian carotenoid cleavage dioxygenases. *Methods in Molecular Biology*, *2083*, 75–88.

von Lintig, J., & Vogt, K. (2000). Filling the gap in vitamin A research. Molecular identification of an enzyme cleaving beta-carotene to retinal. *Journal of Biological Chemistry*, *275*(16), 11915–11920.

Wyss, A., Wirtz, G., Woggon, W., Brugger, R., Wyss, M., Friedlein, A., et al. (2000). Cloning and expression of beta,beta-carotene 15,15′-dioxygenase. *Biochemical and Biophysical Research Communications*, *271*(2), 334–336.